



CITIES WITHOUT A SEISMIC CODE I: HAZARD ASSESSMENT

Kusnowidjaja MEGAWATI¹, Nelson T.K. LAM², Adrian M. CHANDLER³, Tso-Chien PAN⁴

SUMMARY

Most regions located at large distances from plate margins are classified broadly as low- to moderate-seismicity regions. The paper describes approaches that may be followed for seismic hazard assessment of such regions, using Singapore and Hong Kong as examples. Although both cities are considered to be in moderate-seismicity areas, they are exposed to quite different scenarios giving the highest potential seismic threat. The emphasis on a deterministic over a probabilistic approach and *vice versa* are discussed. This is often dictated by the regional seismotectonics. Issues pertaining to the development of attenuation relationships for Singapore and Hong Kong, where the seismic hazards are controlled by distant earthquakes, are examined. The seismic hazards are expressed not only in terms of PGA or PGV, but also in the form of response spectra across a range of natural periods suitable for engineering applications. The design spectra are derived for earthquake scenarios with a range of probability of being exceeded over a certain period of time, corresponding to different performance objectives. Recommendations for other low- to moderate-seismicity regions facing similar issues are also given.

INTRODUCTION

It has been recognized that urban areas located at large distances from tectonic plate margins, broadly categorised as low- to moderate-seismicity regions, may also be affected by earthquake tremors. Singapore and Hong Kong are two examples of such regions in Asia. Seismic resistant designs have yet to be specifically required in the present building codes because structural damage due to earthquakes does not exist in the modern history of the cities. Current building design codes in Singapore and Hong Kong have been developed largely based on the British Standard, which does not have any provision for seismic loading. The potentially damaging earthquakes to these cities, such as a great subduction earthquake (M_w 9.0) in Sumatra and a major intraplate earthquake (M_w 7.4) in the South China coastal region, occurred some 100 years ago, when there were practically no high-rise buildings in the cities.

¹ Research Assistant Professor, Centre for Earthquake Engineering Research, Department of Civil Engineering, The University of Hong Kong. Email: kusno@hkucc.hku.hk

² Senior Lecturer, Department of Civil and Environmental Engineering, The University of Melbourne, Australia. Email: n.lam@civag.unimelb.edu.au

³ Professor and Director, Centre for Earthquake Engineering Research, Department of Civil Engineering, The University of Hong Kong. Email: amchandl@hkucc.hku.hk

⁴ Professor and Director, Protective Technology Research Centre, School of Civil and Environmental Engineering, Nanyang Technological University, Singapore. Email: cpan@ntu.edu.sg

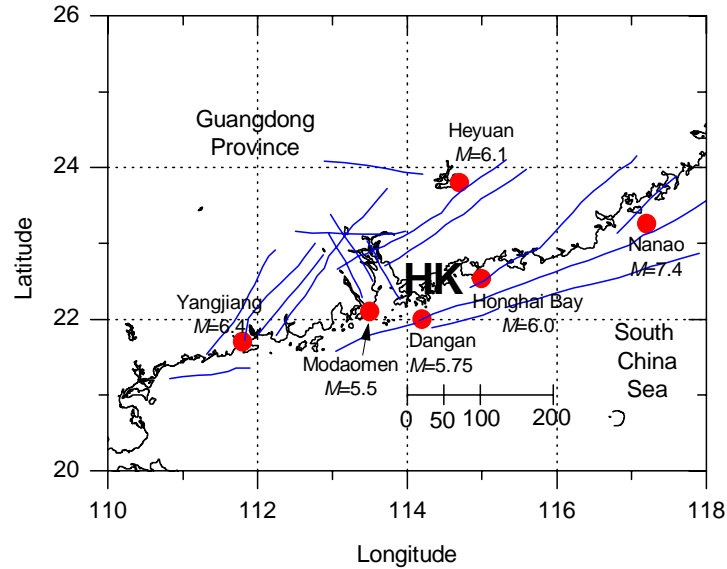


Figure 1. Prominent fault traces in the Hong Kong region with identified historical earthquakes.

In line with the economic growth in Asia, the cities of Singapore and Hong Kong have developed into modern metropolises with large concentrations of population, high-rise buildings, complex infrastructures, and a significant proportion of reclaimed land. Recent earthquakes have frequently shaken high-rise buildings in Hong Kong and Singapore, especially those founded on Quaternary marine clay deposits and reclaimed land. The number of incidents seems to increase as more high-rise structures are built. Therefore, the seismic risk of these cities has increased tremendously compared to their conditions 50 years ago. Although the seismic hazard of the cities may be low due to low seismic activities, the seismic risk, in terms of damage potential to structures, loss of lives, assets, businesses and services, cannot be ignored since structures have not been designed for seismic loads. These cities are two classic examples of areas with low seismic hazard, but with high consequence. This fact warrants thorough seismic hazard assessments for the cities.

The main objective of the present paper is to discuss the approaches and the results of the seismic hazard studies that have been undertaken for these cities. Different approaches have to be applied in seismic hazard assessments of Singapore and Hong Kong because the cities have different seismic environment although both are categorised as low- to moderate-seismicity regions. The present study involves developing new attenuation relationships suitable for the regions, identifying historical and credible future scenario earthquakes, predicting the response spectra due to the identified earthquakes, and evaluating the most appropriate approaches to assess the seismic hazard of other low- and moderate-seismicity regions. It is beyond the scope of the present paper to give detailed descriptions of the methods used in the seismic hazard assessment, as they have been reported elsewhere. Readers are referred to Refs. [1-4] for seismic hazard assessment of Hong Kong and Refs. [5-7] for the case of Singapore. Furthermore, to limit the scope of discussion, this paper presents the seismic hazard on rock sites only.

REGIONAL TECTONIC SETTINGS AND SEISMIC ACTIVITIES

Hong Kong Region

The study area bounded by latitudes 20°N – 26°N and longitudes 110°E – 118°E (Figure 1), is hereafter referred to as the “Hong Kong Region”. Hong Kong is located in South-eastern China, which is considered an intraplate region with moderate seismic activity level. Over the last 1000 years, more than

46 earthquakes with magnitudes greater than 4.75, have occurred within a distance of 350 km from Hong Kong. Eleven of these earthquakes had magnitudes greater than 6 [8]. The city lies within the Southeast coastal seismic belt of China, where four sets of fault zones, trending ENE, NW, EW and NE, have been identified [9]. The ENE-trending Guangdong coastal fault zone is the most significant seismic energy release zone. At least four major earthquakes occurring along this seismic zone have been reportedly felt in Hong Kong: Nanao earthquake in 1600 ($M = 7$, $R = 319$ km), Dangan islands earthquake in 1874 ($M = 5.75$, $R = 30$ km), Honghai Bay earthquake in 1911 ($M = 6$, $R = 85$ km), and Nanao earthquake in 1918 ($M = 7.4$, $R = 338$ km). R indicates the distance from the epicentre to the headquarters of the Hong Kong Observatory (HKO). The 1918 Nanao earthquake caused some minor damage to masonry buildings in Hong Kong, with reported intensities of VI to VII on the Modified Mercalli Intensity (MMI) scale. A series of strong events have occurred along the inland NE-trending zone. The largest ones were the reservoir-triggered Heyuan earthquake in 1962 ($M = 6.1$, $R = 174$ km) and the Yangjiang earthquake in 1969 ($M = 6.4$, $R = 254$ km). The NW- and EW-trending fault zones are of smaller scale. A notable event caused by the NW-trending fault was the earthquake at Modaoemen (Macau) in 1905 ($M = 5.5$, $R = 85$ km). The epicentres of these historical earthquakes are shown in Figure 1.

Besides the intraplate earthquakes described above, Hong Kong has also been affected by large subduction earthquakes in Taiwan and the Philippines. The HKO has recorded 49 events that were felt in Hong Kong since 1980, of which 14 originated from earthquakes in Taiwan (more than 600 km away) and five from the Philippines (more than 700 km away). The remaining 30 events originated from intraplate earthquakes, of which seven occurred within 40 km, 17 events between 40 and 350 km and six events further than 350 km from Hong Kong. This illustrates the complexity of the seismic activity in the region, where the main threats to Hong Kong may arise from major intraplate earthquakes with low probability of occurrence and great interplate earthquakes in the more active region of Taiwan.

Singapore

Singapore is located in a low-seismicity intraplate region. The active seismic sources that may affect the city are located more than 400 km away, along and off the western coast of the island of Sumatra. The Sumatra island is on the Eurasian plate, which overrides the subducting Indian-Australian plate (Figure 2). The convergence along the Sumatran portion of the plate boundary is oblique to the trench axis, with the orientation and magnitude of the relative-motion vector shown in Figure 2. Contradicting the oblique convergence along the Sumatran portion of the subduction zone, slip vectors of moderate earthquakes along this zone were found to be nearly perpendicular to the strike of the plate boundary [10]. It has since been analysed and concluded that a significant amount of the strike-slip component of the oblique convergence between the Indian-Australian plate and the Eurasian plate southwest of Sumatra is accommodated by the right-lateral slips along the trench-parallel Sumatran fault [10].

The largest earthquake that has reportedly happened in the subduction zone is the great 1833 event with M_w estimated between 8.8 and 9.2 [11]. This event ruptured the entire plate margin from the southern island of Enggano to the island of Siberut. The tremor was felt in Singapore, but no damage was reported. Another great event in 1861, with M_w estimated between 8.3 and 8.5, ruptured the entire 300 km long arc segment between Banyak and Pini islands (Figure 2) [12]. This earthquake was felt in the Malay Peninsula and Java. An earthquake with M_w of 7.7 occurred in December 1935 between the rupture zones of the 1833 and 1861 events. The recent Bengkulu earthquake of 4 June 2000, which had an M_w of 7.9 and a hypocentre underneath the Enggano island (Figure 2), caused the strongest tremors that have been felt in Singapore in the last 65 years [13].

The Sumatran fault lies roughly 250 km northeast of the trench. Geological and geophysical evidences identify the fault as a seismically active, right-lateral strike-slip fault [14]. Unlike many other great strike-slip faults, the Sumatran fault is highly segmented. The 1,650-km long fault is composed of 19 major

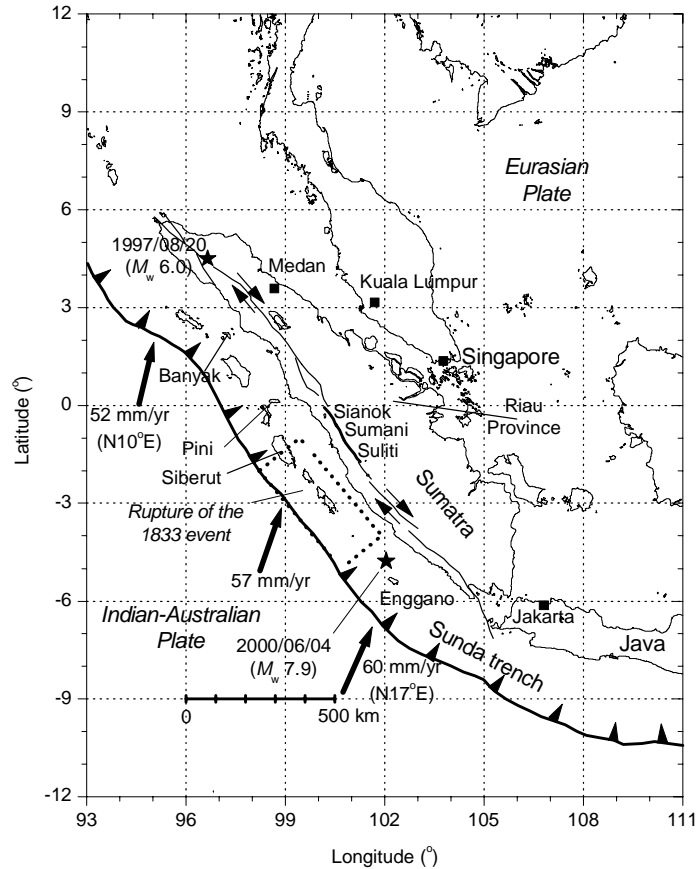


Figure 2. Regional Tectonic setting of Sumatra and the potential seismic source zones considered for seismic hazard assessment of Singapore.

segments with cross-strike width of step-overs between adjacent segments of about 5 to 12 km [14]. The lengths of the segments range from 30 to 220 km. Historical records show that segments of the Sumatran fault have caused numerous major earthquakes but their magnitudes were limited to about 7.5 – 7.7 with rupture lengths not greater than 100 km [14]. The influence of these step-overs on historical seismic source dimensions suggests that the dimension of future events will also be influenced by the fault geometry.

Potential seismic threats for Singapore are likely to arise from great ($M_w > 8$) and major ($M_w > 7$) earthquakes in the distant high-seismicity region of Sumatra. All 17 seismic events reportedly felt in the city since 1971 originated from this region. The earthquakes had magnitude ranging from M_w 5.8 to M_w 7.9. There is no credible report indicating that local earthquakes, within 300 km from the city, have ever generated substantial ground motions capable of causing perceptible levels of shaking.

SEISMIC GROUND MOTIONS RECORDED IN HONG KONG AND SINGAPORE

Seismic Monitoring Networks

A digital seismic monitoring network of eight seismograph stations and three strong motion recorders was installed by HKO in Hong Kong in 1997. The network uses advanced techniques of real-time data transmission and processing, with GPS as the timing standard, to determine the position, depth and magnitude of local and regional earthquakes. The seismic stations are located on rock sites with low background seismic noise. The network has recorded numerous earthquakes, with magnitude between 4

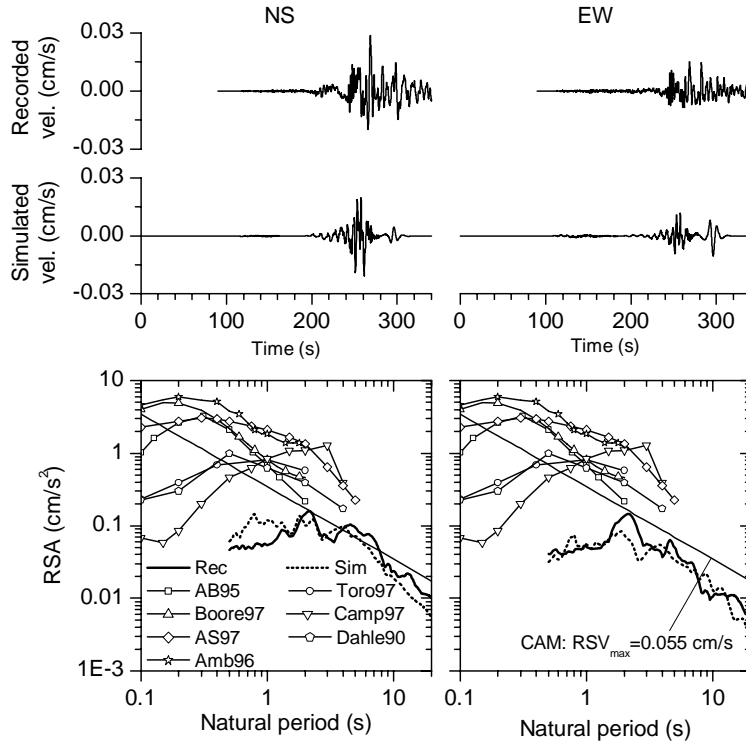


Figure 3. Recorded and simulated ground velocity time histories and acceleration response spectra (5% damping ratio) in Singapore due to the Sumatran-fault event occurring on 20 August 1997 ($M_w = 6.0$, $R = 864$ km).

and 5, in Heyuan, Yangjiang and Nanao. It has also recorded several large earthquakes, with magnitude exceeding 6, in Taiwan and the Philippines.

In Singapore, the Meteorological Service Singapore (MSS) established a network of seismic stations in September 1996, to monitor the regional seismic activities. The network is composed of one broadband Global Seismograph Network (GSN) station, four teleseismic stations and two borehole arrays. The GSN station is situated at the centre of Singapore island, on a rock-outcrop site. From the establishment of the seismic array to December 2001, ground tremors from 37 subduction earthquakes and seven Sumatran-fault events have been recorded by the network.

Recorded Ground Motion of a Distant Earthquake

Figure 3 shows a sample of ground motion recorded at the GSN station of the Singapore network. The ground velocities recorded during a Sumatran-fault event occurring on 20 August 1997 ($M_w = 6.0$, 864 km northwest of Singapore) are shown in the uppermost panels of the figure, where the first and second columns present the NS and EW components. The epicentre of the event is shown in Figure 2. The time 0 s refers to the rupture initiation time, and the records have been baseline corrected and low-pass filtered at 2.0 Hz to remove high-frequency components contaminated by local geology and environmental noises. The acceleration response spectra (5% damping ratio) are depicted by the solid lines in the bottommost panels of the figure.

Evaluation of Existing Attenuation Relationships

Several attenuation relationships have been derived for high-seismicity regions, such as Japan, Western North America (WNA), the Mediterranean margin of Europe, Mexico, and low-seismicity regions, such as

Table I. Description of seven existing attenuation relationships.

Reference	Model notation	Data used	Model type ^a	Region type ^b	M_w^c	R^d (km)
Atkinson and Boore [15]	AB95	Stochastically simulated ground motions in CENA	I	A	4.0 – 7.25	10 – 500
Toro <i>et al.</i> [16]	Toro97	Stochastically simulated ground motions in CENA	I	A	5.0 – 8.0	1 – 500
Boore <i>et al.</i> [17]	Boore97	Recorded ground motions of shallow earthquakes (focal depth ≤ 20 km) in WNA	II	B	5.0 – 7.4	≤ 80
Campbell [18]	Camp97	Recorded ground motions of worldwide earthquakes in active tectonic regions	II	B	≥ 5.0	≤ 60
Abrahamson and Silva [19]	AS97	Recorded ground motions of 58 worldwide shallow earthquakes	II	B	4.4 – 7.5	1 – 220
Dahle <i>et al.</i> [20]	Dahle90	Recorded ground motions of 56 intraplate earthquakes in North America, Europe, China and Australia	II	B	3.0 – 7.8	10 – 1000
Ambraseys <i>et al.</i> [21]	Amb96	Recorded ground motions of earthquakes in Europe	II	B	4.0 – 7.5	≤ 200

^a Type I = attenuation model from curve fitting of stochastically simulated ground motions; Type II = attenuation model from curve fitting of recorded strong motions.

^b Region A = stable continental region; Region B = active tectonic region.

^c M_w indicates the range of moment magnitude considered.

^d R indicates the range of source-to-station distance considered.

Central and Eastern North America (CENA). Most of the existing ground motion relationships, except those for CENA, were derived empirically from large databases of recorded ground motions within distances of around 100 km. They may therefore be valid only within this range. For low-seismicity areas, such as CENA, ground motion relationships have been derived from stochastic ground-motion models. The distance range considered was up to 500 km. Seven attenuation relationships, described briefly in Table I, have been selected to represent the existing ground motion relationships.

The response spectra of the sample ground motion recorded in Singapore are used to examine the appropriateness of extrapolating response spectral estimates given by the existing attenuation relationships to long distance ranges. The bottommost panels of Figure 3 show the comparison between the acceleration response spectra (5% damping ratio) of the Sumatran earthquake and those predicted by the existing ground motion models. The spectra predicted by the ground motion models show great variance among themselves, with Camp97 at the lowest bound and Amb96 at the highest limit. The variance is as large as one order of magnitude in the natural period range of 0.5 – 2.0 s. All the ground motion relationships over-predict the recorded response spectra.

The possible explanations for the discrepancies among the predictions of the existing ground motion models and the over-prediction are the differences in the regional crustal structures and the distance ranges of interest. The extrapolation of the existing attenuation relationships, derived for short distance range, to much longer distance range may lead to incorrect results. Moreover, ground motion relationships are sensitive to regional crustal structures, so that a relationship determined for one tectonic environment

may not be appropriately scaled for use in another tectonic region without remodelling the source and path effects.

DEVELOPMENT OF ATTENUATION RELATIONSHIPS FOR DISTANT EARTHQUAKES

Motivation

Large-magnitude earthquakes generated at long distances are typified by long-period waves, since the high-frequency components have attenuated greatly. The existing attenuation relationships developed in high-seismicity regions are typically based on regression analyses of strong motions recorded in the near field, thus they are not well constrained for the long-distance range. Other attenuation relationships that covered a long-distance range, such as AB95 and Toro97, consistently over-predict the response spectra of distant earthquakes recorded in Singapore. Moreover, the existing attenuation relationships give RSA predictions for a limited natural period range from 0.05 s to 4 s, and when tested for distant earthquakes (Figure 3) most of them reach the peak values in a short-period range of 0.2 – 0.5 s. Seismic waves of such a remote earthquake should be dominated by long-period components (above 1.0 s). This is an indication that the existing attenuation relationships are not intended for ground-motion prediction of distant earthquakes. Response spectrum formats that can effectively represent effects of distant earthquakes are therefore desirable.

The use of ground motion simulation is becoming an increasingly important approach for seismic hazard analyses. This is particularly pertinent in regions where empirical modelling, which is based on regression analysis of previously recorded ground motions, is not feasible because of the inadequate number of recorded motions. Two different methods have been adopted in developing new attenuation relationships for Hong Kong and Singapore. Both methods use seismological models to generate synthetic seismograms that account for source and path effects. The attenuation relationships are derived not only for PGA and PGV, but also for response spectra across a wide range of natural periods suitable for engineering applications.

Component Attenuation Model (CAM)

The first attenuation relationship uses a generic response spectrum prediction model, which is based on stochastic simulations of intraplate earthquakes, taking into account local geophysical properties. This model, called the Component Attenuation Model (CAM) [1,2,22], provides estimates for the maximum values of response spectral acceleration (RSA_{max}), velocity (RSV_{max}) and displacement (RSD_{max}) for both rock and soil sites. These three values are utilised to define the elastic response spectrum over the entire period range of engineering interest. The attenuation relationships are expressed as the product of a source factor $\alpha(M_w)$, a geometrical attenuation factor $G(R,D)$, an anelastic attenuation factor $\beta(R,Q)$, a mid-crust factor and an upper crust factor $\gamma(crust)$. M_w , R , D and Q indicate the moment magnitude, the epicentral distance, the thickness of the crust and the wave transmission quality factor, respectively. The general formulation of CAM for rock sites is given as:

$$\Delta = \alpha(M_w)G(R,D)\beta(R,Q)\gamma(crust) \quad (1)$$

where Δ is the maximum value of the response spectral parameter of interest (RSA_{max} , RSV_{max} or RSD_{max}), and the full descriptions of the attenuation components $\alpha(M_w)$, $G(R,D)$, $\beta(R,Q)$, $\gamma(crust)$ can be found in Refs. [1,4,22].

The stochastic ground motion simulations, on which CAM is based, treat a seismic source as a point source [23]. Therefore, CAM does not consider the source rupture parameters of a specific earthquake, such as the spatial and temporal distributions of the slips on the fault and the fault rupture directivity, but

it models the source parameter as a function of moment magnitude only. This approximation is acceptable when the source-site distance is several times larger than the source size, or the source rupture parameters are not accurately known. CAM is intended to address the fact that attenuation of seismic waves is strongly dependent on regional properties of the earth's crust, through which seismic waves propagate. The crustal influence, relative to the source effects, is expected to be more significant for seismic waves propagating over a long distance.

CAM is used to estimate the response spectrum of the Sumatran earthquake shown in Figure 3. A Q value of 400 and a crustal thickness of 28 km are adopted for the region, based on the Global CRUST 2.0 model [24]. CAM estimates an RSV_{\max} of 0.055 cm/s (shown as solid lines annotated as "CAM" in the figure), which agrees well with the recorded spectra.

Extended Reflectivity Method

The second method uses a theoretical ground-motion simulation procedure called the extended reflectivity method (ERM) [25] that accounts for spatial and temporal distributions of the slips on the fault and complete wave-propagation solutions in a horizontally-layered medium. The ERM approach is applicable for both near-field and far-field earthquakes, as long as reliable representations of source rupture and crustal model are available. When the source-site distance is much larger than the source length, the source may be sufficiently modelled as a single point source. Such model has been used to derive the attenuation relationships for distant Sumatran earthquakes for the purpose of hazard assessment of Singapore and the Malay Peninsula [7]. On the other hand, if the source-site distance is less than two or three times the source length, the rupture process of the fault may play a significant role in determining the intensity of the ground motion at the site. In such a case, the single point-source model may not be appropriate, and the source should be modelled as a propagating fault (multi-point source model). This is not only the case for near-field earthquakes, but also for distant earthquakes with very large magnitude, such as the 1833 Sumatran-subduction earthquake [6]. The rupture length of the earthquake was approximately 500 km, and Singapore was located within 1.5 times the source length.

The ground motions of the Sumatran earthquake shown in Figure 3 have been simulated using ERM (refer "sim" in the figure legend). Both the simulated and recorded velocity time histories in the NS and EW directions and also shown in the upper part of Figure 3. The source is modelled as a point source with a depth of 20 km. The strike, dip and rake angles, as obtained from the Harvard Centroid Moment Tensor (CMT) catalog [26], are N150°E, 87° and -165°, respectively. This indicates a right-lateral strike-slip earthquake. The source rise time is calculated to be 2.85 s, assuming a stress-drop of 100 bars. The regional crustal structure of Sumatra is modelled as a horizontally-layered medium, where the crustal properties have been extracted from the global crustal model CRUST 2.0 [24]. The upper cut-off frequency of the simulation is 2.0 Hz. The simulated waveforms appear to agree substantially well with the recorded data, except that the duration of recorded ground motions appears to be longer than that of the simulated ones. This may be due to the scattering caused by small-scale heterogeneities that cannot be simulated by the one-dimensional layered model. The acceleration response spectra (5% damping ratio) of the simulated and recorded ground motions are compared in the bottommost panels of Figure 3, which show good agreement. The simulated response spectra are in better agreement with the recorded spectra than those predicted by the existing attenuation models.

The agreement found in the simulations of the Sumatran earthquake may imply that the regional crustal structures extracted from CRUST 2.0 [24] can well represent the actual crustal structure of the region studied. It also indicates the capability of ERM to fully simulate the recorded data.

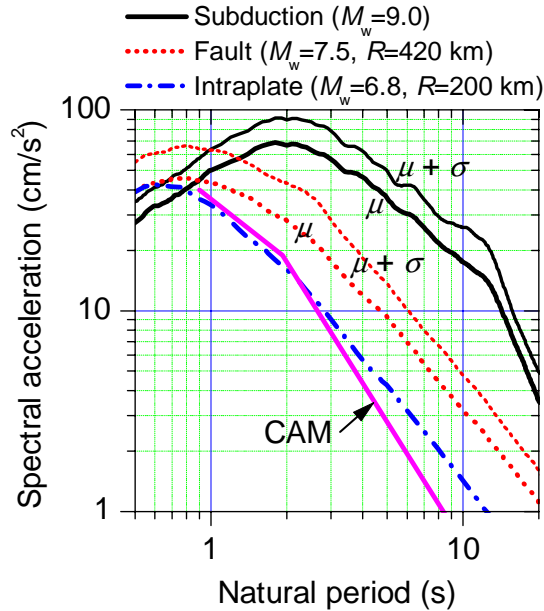


Figure 4. Acceleration response spectra (5% damping ratio) of several earthquake scenarios affecting Singapore.

DETERMINISTIC VERSUS PROBABILISTIC SEISMIC HAZARD ASSESSMENT

Most regions located at large distance from tectonic plate margins are considered as low- to- moderate seismicity regions, due to the moderate level of local seismic activity. These regions may further be divided into two broad categories according to the origin of the most likely damaging seismic sources. The first category describes regions with low local seismicity, where the likely threat arises from great ($M_w > 8$) and major ($M_w > 7$) earthquakes in distant high-seismicity regions. Singapore and the Malay Peninsula are two examples of this category. The second category covers regions with low to moderate local seismic activity levels, with the major threat arising from strong local earthquakes and major distant intraplate earthquakes, both of which have low probability of occurrence. Examples include Hong Kong and CENA. The differences in seismic environment of these two categories lead to different approaches adopted for the seismic hazard assessments, as discussed below.

Seismic Hazard Assessment of Singapore

The seismic hazard assessment conducted for Singapore is rather straightforward using a deterministic approach, where the hazard is controlled by the maximum credible earthquakes occurring along the Sumatran-fault segments closest to Singapore, and along the Sumatran-subduction zones that have capability to generate great earthquakes. Large earthquakes in both seismic sources may be able to affect Singapore. The highly segmented Sumatran fault is only capable of producing earthquakes of a limited size, but it is located relatively closer to Singapore. The perpendicular distance from Singapore to the fault is 420 km. The Subduction zone is located about 250 km further away from the fault, but it has the capability of generating much larger earthquakes with M_w as large as 9.0 [11].

Of the 19 segments of the Sumatran fault, three segments from 2° S to the Equator are closest to Singapore. They are named the Suliti segment ($1.75^\circ\text{S} - 1.0^\circ\text{S}$, length = 95 km), Sumani segment ($1.0^\circ\text{S} - 0.5^\circ\text{S}$, length = 60 km) and Sianok segment ($0.7^\circ\text{S} - 0.1^\circ\text{N}$, length = 90 km) [14], and are highlighted in Figure 2. Two major earthquakes occurred in these segments in the last 100 years. The first one was on 4 August 1926 (M_S estimated about 7) and the second one was on 9 June 1943 ($M_S = 7.4 - 7.6$). Judging

from the length of the segments, the maximum credible magnitude that could be generated by these segments is hypothesised to be 7.5.

Bedrock motions in Singapore due to the 1833 Sumatran subduction earthquake have been simulated using ERM, taking into account uncertainties in source rupture process [6]. Two hundred random rupture models, considering the variations in rupture directivity, slip distribution, presence of asperities, rupture velocity and dislocation rise time, have been generated based on a range of seismologically possible models. Figure 4 shows a pair of horizontal response spectra simulated for this earthquake, namely the mean spectrum (μ) and the mean-plus-one-standard-deviation spectrum ($\mu+\sigma$). The standard deviation accounts for the uncertainties in the source rupture parameters. The spectrum in the figure is represented by the largest spectrum between the spectra in the fault-normal and fault-parallel directions. In the natural period range of 0.5 – 1.6 s, the acceleration response increases with the increase of the natural period. The peak spectral accelerations of about 3 times the PGA are reached within the period of 1.6 – 2.5 s. As the natural period increases further, the spectral accelerations gradually decrease. This period range of 2.5 – 12.5 s is the range where the velocity response spectra level off at a peak value. For a natural period longer than 12.5 s, the response spectra converge to a peak spectral displacement.

The acceleration response spectra (Figure 4) of an M_w 7.5 Sumatran-fault earthquake located closest to Singapore ($R = 420$ km) are estimated using the newly developed attenuation relationships for Sumatran-fault earthquakes [7]. A pair of μ and $\mu+\sigma$ spectra are shown, where the standard deviation accounts for the uncertainties in the rupture parameters, such as the stress drop, focal depth, dip and rake angles. The RSA has the maximum value when the natural period is between 0.6 and 1.0 s, which is shorter than the range associated with the subduction earthquake. This is attributed to the fact that the Sumatran-fault earthquake is located closer to Singapore and has lower magnitude. The comparison of the spectra of these two earthquakes indicates that the spectrum of the subduction earthquake is larger than that of the fault earthquake, except for natural periods lower than 1.0 s. Thus, the subduction earthquake is the most critical for structures with natural periods longer than 1.0 s, which is the case for the majority of residential and office buildings in Singapore.

These two scenarios indicate the maximum magnitudes that may occur in the respective seismic sources. Thus, the spectra may correspond to the performance objective levels of life safety and collapse prevention. The magnitudes of events having shorter return periods need to be identified further, in order to derive design spectra associated with the performance objective levels of fully operational and immediate occupancy. However, it is noteworthy that an earthquake with $M_w \leq 6.8$ in the nearest Sumatran-fault segments or with $M_w \leq 7.5$ in the nearest Sumatran-subduction zone may not be able to generate RSA greater than 15 gal within a natural period range of 0.5–2 s [7]. The threshold of 15 gal is taken from the requirement of the current building code, which stipulates that structures should be capable of resisting a notional horizontal design load equal to 1.5% of the characteristic dead weight.

De-aggregation of PGA in Singapore estimated using a probabilistic seismic hazard analysis (PSHA) indicates that the main contributions come from earthquakes with magnitude greater than 7 along several Sumatran-fault segments located closest to Singapore [5]. A more recent analysis [7] has also indicated that only Sumatran-fault segments located between -3°S and 1°N have the capability to cause RSA greater than 15 gal at natural periods from 1 to 2 s. This shows that even if PSHA is applied for Singapore, the de-aggregation of the results would lead to the two controlling sources, namely the Sumatran-fault segments and subduction zones located closest to Singapore. It is sometimes not necessary to conduct PSHA to identify the most dominant seismic sources for low-seismicity regions where the potential threats arise mainly from distant seismically active regions.

Table II. Magnitude and distance combinations of design-level earthquakes for Hong Kong, for various probabilities of exceedance (PE) in 50 years, with the magnitudes of the corresponding maximum credible earthquakes (MCE) [3]

R (km)	PE = 50%	PE = 10%	PE = 5%	PE = 2%	MCE magnitude
36	-	5.2	5.5	5.8	6.4
90	5.1	5.9	6.2	6.5	6.9
125	5.6	6.3	6.5	6.7	7.2
180	6.0	6.7	7.0	7.2	7.5
280	6.7	7.4	7.6	7.8	8.0
330	6.8	7.4	7.6	7.8	8.0

PE of 50%, 10%, 5% and 2% in 50 years correspond to performance objective levels of Immediate Occupancy, Life Safety, Structural Stability and Collapse Prevention, respectively.

Besides the two very active seismic sources, Singapore may also be affected by moderate-magnitude intraplate earthquakes. More than 20 intraplate earthquakes have occurred in Riau Province of Indonesia, along the eastern coast of Sumatra (Figure 2), in the last 30 years. The largest magnitude reported is m_B 4.6. The seismic environment and the maximum credible magnitudes of earthquakes in this region are largely unknown. The mean response spectrum associated with an M_w 6.8 earthquake in this region, approximately 200 km from Singapore, is estimated using the same attenuation relationship as above. Figure 4 shows that within the period range of common engineering interest from 0.5 to 3.0 s, the acceleration response due to the intraplate earthquake is smaller than those corresponding to the Sumatran-fault and subduction earthquakes. Thus, intraplate earthquakes in this region would cause less significant impacts to Singapore if the maximum credible magnitude is confined below 6.8. However, further investigations should be conducted to understand the movement potential of the faults in this region. The response spectrum of the intraplate earthquake estimated using CAM is also shown in Figure 4. A Q factor of 400 and a crustal thickness of 28 km were adopted. The CAM spectrum shows good agreement with that estimated using the attenuation relationship derived specifically for the Sumatran earthquakes.

Seismic Hazard Assessment of Hong Kong

Seismic hazard assessment of Hong Kong is a more complex issue because the potential seismic sources and fault traces are scattered within a broad region (Figure 1). This complexity warrants a comprehensive probabilistic analysis of earthquake recurrence in the region. A careful study of the seismic data in the Hong Kong region shows that the seismic activity, especially for large magnitude earthquakes, in the far-field region of Hong Kong is significantly higher than that of the near-field, thus the whole region may not be assumed to have uniform seismic activity rate [3]. This leads to the question of what combinations of M_w and R in near-field and far-field regions should be considered appropriate for design of structures in Hong Kong to meet different performance objective levels, such as fully operational, immediate occupancy, life safety and collapse prevention. In other words, what levels of M_w should be assigned in near-field and far-field regions for earthquakes with different levels of probability of being exceeded in, for example, 50 years corresponding to the different performance objectives? The design level of M_w for very low probability of exceedance (or very long return period) should, however, be limited by the maximum credible earthquake magnitude based on the geological conditions of each region. Such analysis has been conducted using a newly proposed method called the Expanding Circular Disk (ECD) [3], and the resulting design M_w and R combinations are given in Table II. Based on these results, the historical 1918 Nanao and 1911 Honghai Bay earthquakes may be associated with earthquakes that have 10%

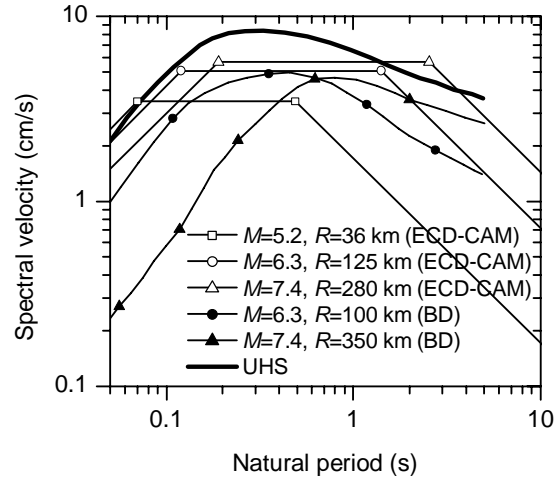


Figure 5. Velocity response spectra (5% damping ratio) of earthquake scenarios affecting Hong Kong, with 10% probability of exceedance in 50 years.

probability of being exceeded in 50 years, whilst the 1874 Dangan islands earthquake may correspond to an earthquake with 2% probability of being exceeded in the same period of time.

The corresponding velocity response spectra of the design earthquake scenarios for different return periods have been estimated using CAM [4]. Figure 5 shows the spectra of three scenario earthquakes with 10% probability of being exceeded in 50 years. The response spectra vary significantly in shape, depending on the earthquake magnitude and distance. The period ranges of the flat parts (the maximum values) of the velocity response spectra correspond with the period range of normal civil-engineering structures. The velocity response spectra associated with distant earthquakes pertain to the critical design cases. For example, the RSV_{max} of the far-field earthquake (e.g. $R = 280$ km) is approximately twice that of the near-field counterpart (e.g. $R = 36$ km).

Another approach for seismic hazard assessment of Hong Kong is by utilising the conventional PSHA, which may be viewed as inclusive of all deterministic events with a finite probability of occurrence. The results of PSHA are typically presented in the form of Uniform Hazard Spectra (UHS) for different levels of probability of being exceeded in a certain period of time. Such an approach has been employed in a consultancy study commissioned by the Buildings Department (BD) of the Government of the Hong Kong Special Administrative Region (HKSAR). The velocity UHS for 10% probability of being exceeded in 50 years is presented in Figure 5. The UHS is somewhat higher than the spectra of the scenario earthquakes estimated by ECD-CAM. This outcome is expected, because the ECD-CAM spectra represent deterministic values based on mean values, whereas the UHS includes an allowance for variability in the predictions of the attenuation relationships used. To be more conservative, the predictions by ECD-CAM may be represented by the mean-plus-one-standard-deviation spectra. Note, all response spectrum predictions shown in Figure 5, including ECD-CAM, BD and UHS are based on results generated from the earthquake simulation program GENQKE [23].

The principal advantage of PSHA is that all possible earthquake occurrences that may contribute to a particular level of the ground-motion hazard are accounted for. The disadvantage is that no single earthquake, in terms of magnitude and distance, is likely to produce a ground motion matching the uniform hazard spectrum at all structural periods. The ground-motion time history is essential in non-linear structural dynamic analysis, which determines the seismic risk evaluation. This disadvantage can be

overcome by de-aggregating all possible earthquake occurrences that contribute to the ground-motion hazard at any particular period. This enables the relative likelihood of an individual earthquake giving rise to the ground motion at that period to be determined. The most likely event can then be derived.

The de-aggregation of the PGA indicates that potential earthquakes at relatively close distance contribute most to the hazard level of Hong Kong. Possible earthquakes at distances greater than 150 km make relatively little contribution to PGA. On the other hand, the de-aggregation of the 2.0-second and 5.0-second RSA indicates that the contribution from earthquakes at distances larger than 150 km, including the Taiwan seismic zone, is much larger than the contribution from near-distance earthquakes. Therefore, for each level of probability of exceedance two or three scenario earthquakes, corresponding to near, intermediate and long distances, may have to be considered.

The de-aggregation of the UHS, shown in Figure 5, at natural periods of 0.4 and 1.0 s result into two dominant earthquake scenarios, namely a magnitude 6.3 event at 100 km and a magnitude 7.4 event at 350 km, respectively. The resulting earthquake scenarios agree substantially with the scenarios estimated using ECD (Table II). This is encouraging given the quite fundamental differences in the approaches used. The response spectra of these two scenarios, calculated using a weighted combination of several attenuation relationships employed in the BD study, are also shown in Figure 5. These spectra are comparable with the spectra predicted by ECD-CAM, except that the RSA of the former are smaller than that of the latter, especially for the long-distance case.

Options Available for Low- to Moderate-Seismicity Regions

The approaches that may be applied in seismic hazard assessment of low- to moderate-seismicity regions depend very much on the completeness of the regional earthquake catalogs and the seismotectonics of the regions. If a region has no or far-from-complete earthquake catalogs, PSHA may not be possible. Thus, the hazard assessment should follow a deterministic approach using earthquake scenarios based on the geological conditions, such as fault length, fault movement potential and historical earthquake records. If the regional earthquake catalogs are mostly complete, PSHA may serve as the best option. De-aggregation of seismic hazard may allow identification of events (magnitudes and distances) that dominate the seismic hazard. These dominant events may then be used to refine the hazard levels.

The most comprehensive seismic hazard assessment may be achieved through recursive analysis, where probabilistic analysis is used to identify dominant deterministic events, and more sophisticated models of these events are then created to account for the variance in the source parameters, such as rupture directivity. The hazard analysis is then repeated with the higher level of detail. For regions in the first category described above, such as Singapore, the dominant events may sometimes be identified without conducting PSHA followed by de-aggregation. The largest earthquakes may occur every 100 to 300 years in the Sumatran seismic source zones, thus earthquakes with 10% probability of being exceeded in 50 years may correspond to the largest magnitudes on the closest faults to the site. Ground motion simulations of the controlling events may then be conducted to estimate the design response spectra [6,7]. For regions with seismic environment falling into the second category described above, the probabilistic approach may be the most appropriate, provided the earthquake catalog is sufficiently complete. However, design earthquake scenarios that contribute mainly to the probabilistic ground motion parameters should be identified, and dynamic analyses of structures must be based on the identified earthquake scenarios.

CONCLUSIONS

Although Singapore and Hong Kong are both located in moderate-seismicity regions, they are exposed to quite different scenarios of the most potential seismic threats. The characteristics of the seismic sources resulted into two different approaches being adopted for the seismic hazard assessments of the cities. The

potential seismic threats for Singapore largely arise from distant but very active Sumatran seismic source zones, whilst no moderate earthquake with magnitude greater than 5 has ever been reported within 300 km from the city. This fact made the deterministic approach more appealing, where the response spectra in Singapore due to the maximum credible earthquakes along the Sumatran fault and the subduction zone were predicted using a theoretical ground motion simulation procedure (ERM). The ground motion simulations included an allowance for variability in the source rupture parameters. On the other hand, the potential seismic sources and fault traces that may affect Hong Kong are scattered within a broad region, which make the probabilistic approaches more appropriate in the hazard assessment. Several combinations of M_w and R have been considered in near field and far field of Hong Kong to meet different objective levels suitable for performance-based structural designs. The design spectra have then been computed using the conventional PSHA and the newly developed ECD-CAM. Options available for other low- to moderate-seismicity regions facing similar problems have also been described.

To make the discussion on the seismic hazard and risk of low- to moderate-seismicity regions more complete, the present paper is followed by a companion paper [27], which deals with seismic risk assessment and development of rational seismic codes for such regions.

ACKNOWLEDGEMENTS

The authors would like to thank the Buildings Department of the Government of the Hong Kong Special Administrative Region (HKSAR) for their permission to allow the inclusion of selected results from their seismic hazard study. The work pertaining to Hong Kong was substantially supported by a grant from the Research Grants Council of the HKSAR (Project No. HKU 7004/02E), whose support is gratefully acknowledged. The ground motion of the Sumatran earthquake in Figure 3 was kindly provided by the Meteorological Service Singapore (MSS). The first author would like to thank Professor Kazuki Koketsu of Earthquake Research Institute, the University of Tokyo, for fruitful discussions in several occasions.

REFERENCES

1. Lam NTK, Wilson JL, Chandler AM, Hutchinson GL. "Response spectral attenuation relationships for rock sites derived from the component attenuation model." *Earthquake Engineering and Structural Dynamics* 2000; 29: 1457-1489.
2. Lam NTK, Wilson JL, Chandler AM, Hutchinson GL. "Response spectrum modelling for rock sites in low and moderate seismicity regions combining velocity, displacement and acceleration predictions." *Earthquake Engineering and Structural Dynamics* 2000; 29: 1491-1525.
3. Chandler AM, Lam NTK. "Scenario predictions for potential near-field and far-field earthquakes affecting Hong Kong." *Soil Dynamics and Earthquake Engineering* 2002; 22: 29-46.
4. Lam NTK, Chandler AM, Wilson JL, Hutchinson GL. "Response spectrum predictions for potential near-field and far-field earthquakes affecting Hong Kong: rock sites." *Soil Dynamics and Earthquake Engineering* 2002; 22: 47-72.
5. Pan TC, Megawati K. "Estimation of peak ground accelerations of the Malay Peninsula due to distant Sumatra earthquakes." *Bulletin of Seismological Society of America* 2002; 92: 1082-1094.
6. Megawati K, Pan TC. "Prediction of the maximum credible ground motion in Singapore due to a great Sumatran subduction earthquake: the worst-case scenario." *Earthquake Engineering and Structural Dynamics* 2002; 31: 1501-1523.
7. Megawati K, Pan TC, Koketsu K. "Response spectral attenuation relationships for Singapore and the Malay Peninsula due to distant Sumatran-fault earthquakes." *Earthquake Engineering and Structural Dynamics* 2003; 32: 2241-2265.
8. Geotechnical Control Office. "Review of earthquake data for the Hong Kong region." Geotechnical Control Office, Civil Engineering Service Department, Hong Kong, Publication No. 1, 1991.

9. Lee CF, Ye H, Zhou Q. "On the potential seismic hazard in Hong Kong." *Episodes* 1997; 20(2): 89-94.
10. McCaffrey R. "Oblique plate convergence, slip vectors, and forearc deformation." *Journal of Geophysical Research* 1992; 97(B6): 8905-8915.
11. Zachariassen J, Sieh K, Taylor FW, Edwards RL, Hantoro WS. "Submergence and uplift associated with the giant 1833 Sumatran subduction earthquake: Evidence from coral microatolls." *Journal of Geophysical Research* 1999; 104: 895-919.
12. Newcomb KR, McCann WR. "Seismic history and seismotectonics of the Sunda Arc." *Journal of Geophysical Research* 1987; 92: 421-439.
13. Pan TC, Megawati K, Brownjohn JMW, Lee CL. The Bengkulu, Southern Sumatra, earthquake of 4 June 2000 ($M_w = 7.7$): Another warning to remote metropolitan areas. *Seismological Research Letters* 2001; 72(2): 171-185.
14. Sieh K, Natawidjaja D. "Neotectonics of the Sumatran fault, Indonesia." *Journal of Geophysical Research* 2000; 105: 28295-28326.
15. Atkinson GM, Boore DM. "Ground-motion relations for Eastern North America." *Bulletin of the Seismological Society of America* 1995; 85: 17-30.
16. Toro GR, Abrahamson NA, Schneider JF. "Model of strong ground motions from earthquakes in Central and Eastern North America: best estimates and uncertainties." *Seismological Research Letters* 1997; 68: 41-57.
17. Boore DM, Joyner WB, Fumal TE. "Equations for estimating horizontal response spectra and peak acceleration from Western North American earthquakes: a summary of recent work." *Seismological Research Letters* 1997; 68: 128-153.
18. Campbell KW. "Empirical near-source attenuation relationships for horizontal and vertical components of peak ground acceleration, peak ground velocity, and pseudo-absolute acceleration response spectra." *Seismological Research Letters* 1997; 68: 154-179.
19. Abrahamson NA, Silva WJ. "Empirical response spectral attenuation relations for shallow crustal earthquakes." *Seismological Research Letters* 1997; 68: 94-127.
20. Dahle A, Bungum H, Kvamme LB. "Attenuation models inferred from intraplate earthquake recordings." *Earthquake Engineering and Structural Dynamics* 1990; 19: 1125-1141.
21. Ambraseys NN, Simpson KA, Bommer JJ. "Prediction of horizontal response spectra in Europe." *Earthquake Engineering and Structural Dynamics* 1996; 25: 371-400.
22. Chandler AM, Lam NTK. "An attenuation model for distant earthquakes." *Earthquake Engineering and Structural Dynamics* 2004; 33: 183-210.
23. Lam NTK, Wilson JL, Hutchinson GL. "Generation of synthetic earthquake accelerograms using seismological modelling: a review." *Journal of Earthquake Engineering* 2000; 3: 321-354.
24. Global Crustal Model CRUST 2.0. Institute of Geophysics and Planetary Physics, The University of California, San Diego website: <http://mahi.ucsd.edu/Gabi/rem.dir/crust/crust2.html>.
25. Kohketsu K. "The extended reflectivity method for synthetic near-field seismograms." *Journal of Physics of the Earth* 1985; 33(2): 121-131.
26. Harvard Seismology Centroid Moment Tensor Database. Department of Earth and Planetary Sciences, Harvard University website: <http://www.seismology.harvard.edu/CMTsearch.html>.
27. Lam NTK, Pan TC, Chandler AM, Megawati K. "Cities without a seismic code II: codification and risk assessment." *Proceedings of the 13th World Conference on Earthquake Engineering*, Vancouver, Canada. Paper No. 141 (CD-ROM).